SIMLIDAR – Simulation of LIDAR performance in artificially simulated orchards

Valeriano Méndez[a, c, d], Heliodoro Catalán[a], Joan R. Rosell[b], Jaume Arnó[b], Ricardo Sanz[b], Ana Tarquis[a]

[a] Department of Applied Mathematics. Agronomic E.T.C., Polytechnic University of Madrid**.** Ciudad Universitaria s/n, 28040 – Madrid, Spain.

[b] Department of Agro-forestry Engineering, University of Lleida, Avinguda Rovira Roure, 191, 25198 Lleida, Spain.

[c] Corresponding author. Telephone.: +34 917 308 355; Mobile Number: +34 616 981 407. E-mail addresses: valeriano.mendez@upm.es; v.mendez@grupobbva.com (V. Méndez), h.catalan@upm.es (H. Catalán).

[d] Proofs Correspondence. Valeriano Méndez. Dpto. Matemática Aplicada. E.T.S. Ingenieros Agrónomos. Universidad Politécnica de Madrid. Ciudad Universitaria s/n, 28040 – Madrid. E-mail: valeriano.mendez@upm.es; v.mendez@grupobbva.com.

ABSTRACT

SIMLIDAR is an application developed in C++ that generates an artificial orchard using a Lindenmayer system. The application simulates the lateral interaction between the artificial orchard and a laser scanner or LIDAR (Light Detection and Ranging). To best highlight the unique qualities of the LIDAR simulation, this work focuses on apple trees without leaves, i.e. the woody structure. The objective is to simulate a terrestrial laser sensor (LIDAR) when applied to different artificially created orchards and compare the simulated characteristics of trees with the parameters obtained with the LIDAR. The scanner is mounted on a virtual tractor and measures the distance between the origin of the laser beam and the nearby plant object. This measurement is taken with an angular scan in a plane which is perpendicular to the route of the virtual tractor. SIMLIDAR determines the distance measured in a bi-dimensional matrix N×M, where N is the number of angular scans and M is the number of steps in the tractor route. In order to test the data and performance of SIMLIDAR, the simulation has been applied to 42 different artificial orchards. After previously defining and calculating two vegetative parameters (wood area and wood projected area) of the simulated trees, a good correlation (R^2=0.70-0.80) was found between these characteristics and the wood area detected (impacted) by the laser beam. The designed software can be valuable in horticulture for estimating biomass and optimising the pesticide treatments that are performed in winter.

KEYWORDS

LIDAR, Lindenmayer system, simulation, orchards.

49

Variable	***Description***
a, b, c	A point of mesh that model the laser beam, taken a, b, c values from 1 to P + 1.
A_{IM}	Impacted area, m^2.
A_{PR}	Projected wood area, m^2.
d	Diameter of a branch.
d_m	Minimum branch diameter.
$\Delta\theta$	Angle increase between two scan.
Δr	Distance increase along the laser beam.
Δy	Cross-sectional advance increase of the tractor.
$\overrightarrow{H}$	Turtle's heading.
h	Height of a cylindrical branch.
h_0	Height of the axiom branch.
i^{th}	Generation cycle in an L-system substitutions process.
$\overrightarrow{L}$	Turtle left direction.
Laser beam	One of the beams in a 'scan'
l_{ij}	Measured distance where i = 1, …, N and j = 1, …, M, given that N is the number of angular scans and M is the number of steps in the tractor route.
n	Number of branches.
Nb	Number of active buds
n_i	Number of branches in the i^{th} substitution.
Ns	Number of substitutions or production done in the L-system.
P	Precision used to determinate a three dimensional mesh that model the laser beam. The number of points of the mesh is $(P+1)^3$.
θ	The angle of a particular sampling beam in the scan , separated by $\Delta\theta$ from the previous scan
r	Distance along the laser beam.
S	Production or sequence of substitutions in a L-system.
Scan	A vertical sweep done with the scan.
$\overrightarrow{U}$	Turtle up direction.
V_L	Wood volume.
Ω	The alphabet of the L-system.
W	Initial axiom in a L-system.
x	The lateral distance, from the scanner positioned in the interrow, in the model.
x_0	The distance of the laser in front of the ground.
y	Cross-sectional advance in the OY axis.
z	Height coordinate in the model.
z_0	The height of the laser above the ground.

INTRODUCTION

Light detection and ranging (LIDAR) is an active remote sensing technique that uses a laser beam for different applications. The LIDAR measures the distance between the sensor and a target, based on two methods. Measurement of this distance can be based either on the time which elapses between the emission and the return of laser pulses (time-of-flight method) or on trigonometry (optical-probe or light-section methods) in order for 3-D information about the target to be obtained. In the case of portable ground-based applications, scanning is commonly used for the measurements because it allows more efficient data collection than the non-scanning alternative **(**Henning and Radtke, 2006**;** Hosoi and Omasa, 2006**).**

The use of LIDAR in agriculture is relatively recent. Among the most interesting applications are canopy measurements of different trees (Brandtberg et al., 2003**;** Parker et al., 2004**;** Holmgren and Persson**,** 2004**;** Omasa *et al*., 2007**;** Hosoi *et al*., 2005**;** Hosoi and Omasa, 2006**;** Maltamo *et al*., 2004**;** Lefsky *et al*., 1999**;** Riaño *et al*., 2004), the evaluation of vegetative parameters in tree crops (Tumbo *et al*., 2002; Wei and Salyani, 2004 and 2005) and herbaceous crops (Tucker *et al*., 1985; DeFries *et al*., 1999), the obtaining of 3-D images of trees (Rosell *et al.*, 2009a), the estimation of the foliar surface area in fruit trees and vineyards (Rosell *et al.*, 2009b; Arnó *et al*., 2006; Palacín *et al*., 2007), the development of agricultural robots (Monta *et al*., 2004), and its use as a navigational sensor in automatic-guided systems in tractors and agricultural machinery (Mizrach *et al.*, 1994; Chateau *et al*., 2000; Subramanian *et al*., 2006; Barawid *et al*., 2007). However, in the existing scientific literature there is very little information which addresses the technical characteristics and the real potential of this type of commercial sensor (Lee and Ehsani, 2007).

LIDAR technology has become an excellent piece of equipment for the rapid geometric parameterisation of trees and for determining the indexes or vegetative parameters of a tree. Walklate *et al*., (1997 and 2002) offer an interesting methodology to calculate diverse geometric parameters and structures in apple trees. They obtain this data by means of the probabilistic interpretation of the light emitted by the sensor when it interacts with vegetation. However, the methodology proposed by Walklate *et al.* (2002) does not seem to be the most appropriate for crops with high vegetative density (those which make it difficult for light to penetrate), which occurs with some types of citrus crops and certain cereal crops. Nevertheless, the use of LIDAR in field tests is necessary for the characterisation of trees in the absence of a vegetation simulator. To solve this problem, it would be useful to have a software application capable of simulating simultaneously the trees and the operation of the LIDAR. The main goal of this study has been to develop a computer application (SIMLIDAR) that allows the simulation of a terrestrial laser sensor (LIDAR) when applied to different artificially created orchards, and compare the simulated characteristics of trees with the parameters obtained with the LIDAR. Working initially with leafless trees, the aim was to test whether the wood area detected (impacted) by the LIDAR correlates well with the total wood area (or volume) of virtual orchards.

Tarquis, Méndez and Walklate et al. (2006) introduced a new methodology for estimation of the laser target area of an orchard. The final result of the process is a target

distance matrix and its bi-dimensional graphic. In this initial work two independent processes were used, one to obtain the orchard model from an L-system and the other to obtain the laser target area. In the current work all the tasks have been integrated into a single system, which is used to obtain both the orchard model and the subsequent laser target area estimation. In addition, the vegetative measures have been extended and a study undertaken of the correlations between them. The architecture of the process has been designed to allow new plant objects such as leaves to be included, as well as other kinds of plants, such as the vine.

A laser scanner measures the distance to a group of objects over various dimensions (advance direction, transversal sweep, and angular sweep). The computer application SIMLIDAR (acronym for LIDAR simulation) generates an orchard and obtains a simulation of the LIDAR operation giving the value of the distance in each laser position. Instead of simulating a stochastic laser beam interception, as proposed by Kim (2009), a non-stochastic interception is used. In order to verify its results more accurately, SIMLIDAR has initially been used to study apple tree orchards which only have a wood structure. For the generation (simulation) of trees, several authors have used the Lindenmayer system (L-system) (Lindenmayer 1968; Frijters, 1974; Prusinkiewicz, 1987; Prusinkiewicz et al, 1988; Prusinkiewicz and Hanan, 1990 a; Prusinkiewicz et al, 2000; Costes et al, 2008). This system, suitably adapted to orchards, has also been adopted here. It is expected that SIMLIDAR can be used for diverse applications. Since the software can generate numerical simulations in orchards, it could be very useful for the study of different vegetative measures of interest in fruit growing. One of the objectives of this work was to verify whether the impacted area correlated with the projected area as well as with the total wood area and volume.

MATERIALS AND METHODS

SIMLIDAR is an object-oriented application developed in Microsoft Visual C++ 6.0. It was developed to test the viability of determining the LIDAR indices of a canopy by computer simulation. It generates canopy geometry using a Lindenmayer system (L-system) which makes it possible to obtain a realistic geometry that is variable using different plant parameters (number of iterations, angle, rotation, pruning, radius of the smallest branch). An open L-system model (Tarquis and González-Andrés, 1995; Tarquis et al, 2006) was used to produce a geometric description of the branching pattern for a typical pre-blossom tree structure. In MAppleT, L-systems have been used to simulate an orchard (Costes et al, 2008). The graphic representation of the orchard is shown with a three-dimensional scene developed with the OpenGL™ 1.0 library (OpenGL, 1997 and Rogelberg, 1992), which is included in Visual C++. In addition, generic functions such as zoom, rotation, translation and printing of the scene are also included.

SIMLIDAR provides the distance between the laser beam origin and the nearby plant object. This measurement is calculated by simulating an angular scan over the plane perpendicular to the route of the tractor. A different scan precision can be simulated by changing the parameters. The goal is to have a tool to obtain a numerical simulation of LIDAR scanning in different orchards. These simulations allow rapid verification of the performance of different vegetative measurements without having to wait for expensive

experimental studies. Numerical simulation also enables vegetative measurements to be obtained more easily and with greater precision. The originality of this study lies in the fact that its core work focuses on numerical simulation of LIDAR scanning. An L-system is used to obtain the virtual orchard. In addition, SIMLIDAR is a proprietary development that does not use any third party software except Visual C++.

The LIDAR simulation stores the measured distance in a bi-dimensional matrix (l_{ij}) where i = 1, …, N and j = 1, …, M, with N being the number of angular scans and M the number of steps in the tractor route. This matrix is represented using a two-dimensional graphic with a colour guideline which corresponds to the distance measured.

1 L-system process for generating and modelling artificial orchards

An L-system is a technique for defining complex objects by successively replacing parts of a simple initial object using a set of rewriting rules or productions. A classic example of a graphical object defined in terms of rewriting rules was proposed by von Koch (1905). Using rewriting systems which operate on character strings, Chomsky (1956) introduced the concept of formal grammar. The essential difference between Chomsky grammars and L-systems (Lindenmayer, 1968) lies in the method of applying productions. In Chomsky grammars, the productions are applied sequentially, whereas in L-systems they are applied in parallel and simultaneously replace all letters in a given word. L-system productions can therefore be used to capture cell divisions in multicellular organisms, where many divisions may occur at the same time.

The rewriting process starts from a distinguished string called the axiom. In the first derivation step, each letter of the axiom is replaced according to the productions or substitution rules. The axiom becomes a new word where it will apply the productions in the second and following derivation steps.

The L-system is an alphabetic string, where each letter of the alphabet represents the movement of an imaginary turtle that describes the tree. An iterative substitution process is used to obtain the final string of an L-system. The process starts with an initial axiom which is a short string that represents a budding tree. In each iterative step the active bud is replaced by a new branch structure so, for example, active bud and branch are letters of the alphabet. The final string is translated to a virtual three-dimensional tree following the movement rules of the alphabet. In Table 1, some easy examples of L-system strings are shown.

The virtual production of the plant model has two steps. The first step is to develop a grammar and the second step is to interpret this grammar and produce the final plant model. Sipser (1997) describes the L-System method grammar as a collection of substitution rules or productions. A substitution comprises a symbol, an arrow and a string. The symbol is a single variable, usually represented in capital letters. The string consists of variables (also in capital letters) and other symbols called terminals. The entire set of variables is referred to as the alphabet (Ω) of the system. Terminals can be lowercase letters, numbers or special symbols. The grammar is used to describe a language in the following manner. There is a start variable, called the axiom. This axiom (*w*) initialises a string, where all the substitutions will be done; this string is called the derivation string. The symbol to the left (referred to as the predecessor) of

each substitution rule or production is replaced with the symbol to the right (called the successor) of that rule or production in the derivation string. The symbol is replaced as many times as it appears. This process is completed for each production. The finite set of all productions is known as P. The cycle or sequence of substitutions (S) is performed *n* times to obtain the final derivation string. Each time is referred to as one generation.

Prusinkiewicz and Lindenmayer (1990) define a deterministic L-system as a triplet {Ω, *w*, S}. In order to get a non-stochastic apple tree, SIMLIDAR uses the following L-system grammar:

Alphabet (Ω): {F, I, [,], +, -, R, r}
Axiom (*w*): F
Productions (S): {F → InIn[r+InIn+F]In[R-InF]InF}

The geometric representation of all the variables used in the alphabet is in Table 2. In the productions predecessor there is a terminal, referred to as the *n* terminal, which is the axis order of every branch according to the biological terminology of Reffye (1988). The length of growth units and the thickness of each branch tend to decrease for higher-order axes (Fig 1). The final derivation string for 2 and 3 generation cycles are shown in Table 1. To obtain a more realistic effect, SIMLIDAR obtains the following stochastic L-system grammar, where each production can be selected with approximately the same probability of 1/3.

Alphabet (Ω): {F, I, [,], +, -, R, r}
Axiom (***w***): F
Productions (S):

s_1: F $\xrightarrow{.33}$ InIn[r+InIn+F]In[RR-InF]InF
s_2: F $\xrightarrow{.33}$ In[r+InF]In[rr-InF]In[r+InF]F
s_3: F $\xrightarrow{.33}$ In[r+InF]In[R-InF]In[RR+InF]F

For the i^{th} generation cycle, the following series of mathematical equations were applied: the number of branch elements $n_i = Ns\, Nb^{(i-1)}$ with Ns the number of substitutions or cumulative branch generation, Nb the number of active buds and with length $h_i = \frac{h_0}{2^{(i-1)}}$, where h_0 is the branch element length of the initial axiom. Furthermore, to simulate the detailed geometry of a tree structure, the stick-like branches are replaced by cylinders of diameter $d_i = \frac{Ns\, d_m}{i}$, where d_m is the minimum branch diameter and *m* is the cumulative branch generation.

Turtle geometry (Abelson and diSessa, 1982) is used to interpret the L-System. A turtle is a drawing cursor in 3D with two parameters, that of a position and a heading. The output derivation string, obtained with L-System grammar, contains turtle command as an intrinsic geometry. Every grammar variable is a turtle command (Table 2). The current orientation of the turtle in space is represented by three vectors indicating the turtle's heading ($\vec{H}$), the direction to the left ($\vec{L}$), and the up direction ($\vec{U}$), as described by Abelson and diSessa (1982). $\vec{H}$ rolling is not used in SIMLIDAR since a

cylinder does not change its position by rotating through its central axis. These commands can be used to create topological objects which Prusinkiewicz and Lindenmayer (1990) refer to as axial trees; they are an extension of the rooted trees from graph theory.

Specific C++ classes have been developed to address each object in plant modelling. The three-dimensional scene of plant modelling is represented in SIMLIDAR using the standard Open GL (OpenGL, 1997). The standard Open GL function is implemented to allow the SIMLIDAR desktop to rotate, scale or translate the 3D scene. A tree branch is represented in the model by a cylindrical straight trunk, which is determined by knowing the coordinates in A^3 points ($x_{ini}, y_{ini}, z_{ini}$) and ($x_{fin}, y_{fin}, z_{fin}$), and the diameter *d* of the cylinder. The F variable of the grammar, which represents a leaf in the plant model, is not interpreted by SIMLIDAR in order to allow a more direct testing of the scanning process and because the foliar density of the L-system model could interfere in the results discussion. Finally, an optional pruning process is included in the interpretation step. Assuming that all the down-sloping branches must be pruned, all branches where the position of the turtle descends with respect to the OZ axis are removed.

2 Scanner simulation

The SIMLIDAR application allows for simulation of a laser scanner (LIDAR) applied to virtual plant modelling. It simulates a virtual tractor-mounted LIDAR that advances along the OY axis in the row of the orchard, scanning the plant model in an angular movement in the XZ plane.

The way to simulate the scanning process is by making 3 independent movements. There is a cross-sectional advance along the OY axis from starting point y_1, carrying out successive incremental advances of Δy, given Δy as a parameter of the simulation. There is then an angular advance (θ) at a given position of the OY axis (y_i) between two fixed angular values ($\theta_{\min}$ and $\theta_{\max}$), advancing incrementally by $\Delta\theta$, which is also a parameter of the program. In this case, $\theta_{\min}$ and $\theta_{\max}$ are calculated from the laser beam position and the maximum plant height in each displacement of y_i. Finally, at each position (y_i, θ_k), a virtual laser beam is directed into the orchard and a rectilinear and radial movement is simulated.

When the laser beam reaches an element of the modelled plant, the distance between the modelled plant and the laser origin is stored. If the laser beam is not intercepted by the plant, it may be intercepted by the ground (when $\theta < 0$) or in some cases it may not be intercepted at all (when $\theta > 0$). In the first case the distance to the ground is recorded and in the second case an escape distance is recorded (a constant of SIMLIDAR is used with a distance much greater than any possible interception). The result of the simulation is a matrix L where each $l_{i,k}$ element is the laser beam distance of the plant model in each (y_i, θ_k) laser position. It is possible to represent the measurement obtained by the laser simulation in a two-dimensional graph by selecting different colours for each range of scan distances. The visual matching of the 3D plant model

with the 2D scanning graph representation results in a gross verification of the scan process (Fig 2).

SIMLIDAR supplies other vegetative measurements directly from the virtual plant model: total wood volume, V_L, directly measured from the cylindrical branch model; total wood area, A_L, also directly measured from the cylindrical branch model; projected wood area, A_{PR}, the area of each cylindrical element projected over the current $\vec{L}\times\vec{U}$ plane of the cylinder (Fig 3), or in other words the projection of each branch on a plane facing the LIDAR. When a laser beam hits a branch, the impacted area is considered to be the projection on the YZ plane obtained by the following equation:

$$\Delta y_i \cdot \left[\left(z_0 + l_{ij} \cdot \sin\left(\theta_j + \Delta\theta\right)\right) - \left(z_0 + l_{ij} \cdot \sin\left(\theta_j\right)\right)\right] \quad [1]$$

where z_0 is the height of the laser above the ground, and l_{ij}, θ_i are the distance and the impact angle, respectively. As such, the total detected (impacted) area will be equal to

$$A_{IM} = \sum_{i,j} \Delta y_i \cdot \left[\left(z_0 + l_{ij} \cdot \sin\left(\theta_j + \Delta\theta\right)\right) - \left(z_0 + l_{ij} \cdot \sin\left(\theta_j\right)\right)\right] \quad [2]$$

The tree projected area on the incidence plane is defined as the maximum area that can be impacted in each one of the plant branches. For a cylindrical branch with height ***h*** and diameter ***d***, this area can be measured as $d \cdot h$, and the projected wood area of all the tree's wood structures can be measured as:

$$A_{PR} = \sum_{i=1}^{n} d_i \cdot h_i \text{ or } A_{PR} = \sum_{i=1}^{n} \frac{\pi \cdot d_i^{\,2}}{4} \quad [3]$$

if the base of the cylinder faces the LIDAR. As a result, $A_{IM} \le A_{PR}$. Finally, the area and volume of the wood structure of the cylindrical elements can be measured using the following two formulas:

$$A_L = \sum_{i=1}^{n} \pi \cdot d_i \cdot h_i \quad [4]$$

gives the total wood area, and

$$V_L = \sum_{i=1}^{n} \frac{\pi \cdot d_i^{\,2} \cdot h_i}{4} \quad [5]$$

gives the total wood volume.

2.1 Cross-sectional advance of LIDAR

To obtain the LIDAR measurements with an instrument, a scanning laser beam must cross the orchard in a cross-sectional manner. It is generally understood that this sensor advances along the OY axis (Fig 4). The scanner is positioned in the transversal axis and moves its viewfinder angularly while carrying out a complete sweep of the orchard. The cross-sectional advance along the OY axis takes place in constant increases of Δy after each complete angular sweep. In each iteration *y* increases by a constant value of Δy; in an *i*-iteration we will have a value of *y* equal to:

$$y_i = y_1 + (i-1) * \Delta y \text{ for } i = 1 \cdots N \quad given \quad N = Int\left(\frac{Max(y) - Min(y)}{\Delta y}\right) \quad [6]$$

where N is the number of complete scans performed while the scanner crosses the orchard.

2.2 Angular advance of LIDAR

A full angular sweep θ takes place with constant angular increases between the minimum and maximum angle values. The angular value in the k^{th}-iteration is:

$$\theta_k = \theta_1 + (k-1) * \Delta\theta \text{ for } k = 1 \cdots M \quad given \quad M = Int\left(\frac{Max(\theta) - Min(\theta)}{\Delta\theta} \right) \qquad [7]$$

It is possible to calculate the minimum and maximum value of θ with the following formula (Fig 4):

$$Min(\theta) = \theta_1 = -a\tan\left(\frac{z_0}{Max(x) - x_0} \right)$$

$$Max(\theta) = \theta_M = a\tan\left(\frac{Max(z) - z_0}{Max(x) - x_0} \right) \qquad [8]$$

The number of laser beams is the product of $N \times M$ which defines the matrix L with elements $l_{i,k}$. The laser beam has an angular resolution, $\Delta\theta$, that can be changed in SIMLIDAR by the user. The height of the impact will depend on both $\Delta\theta$ and the impact distance stored in $l_{i,k}$ (equation 14).

2.3 Angular sweeping of LIDAR

For any given position of a simple laser beam (given by y_i, θ_k), any cylindrical branches or objects will be intercepted by the path of the laser beam when $Min(y) \le y_i \le Max(y)$ given that $Min(y)$ and $Max(y)$ are the minimum and maximum of the *y* coordinate and that each considers either the cylindrical objects or the branches.

The $Min(x)$ and $Max(x)$ extremes of the cylinder/branch object project the angle θ_k on the OZ axis at:

$$z_{\min} = z_0 + \frac{x_0 - Min(x)}{\tan(\theta_k)}$$

$$z_{\max} = z_0 + \frac{x_0 - Max(x)}{\tan(\theta_k)} \qquad [9]$$

The cylindrical object or branch object can intersect the direction θ_k when the projection of the *Min(x)* and *Max(x)* ends on OZ (z_{min} and z_{max}) and intersects with the ends of the branch object in the OZ direction (*Min(z)* and *Max(z)*), or if it fulfils either of the following conditions:

$$z_{\min} > Max(z)$$

$$z_{\max} < Min(z) \qquad [10]$$

Based on the projection of the branch outline in the direction θ_k, once it is detected that an intersection could exist (Fig 4), the program executes a radial approach between the two values of the radius (an initial value r_1 and a final value r_P):

$$r_1 = \frac{x_0 - Max(x)}{\cos(\theta_k + \Delta\theta)} \quad Given\ \theta_k > 0$$
$$r_P = \frac{x_0 - Max(x)}{\cos(\theta_k + \Delta\theta)} \quad Given\ \theta_k > 0 \qquad [11]$$

If the value of $\theta_k < 0$, the previous equations are:

$$r_1 = \frac{x_0 - Max(x)}{\cos(-\theta_k)} \quad Given\ \theta_k < 0$$
$$r_P = \frac{x_0 - Max(x)}{\cos(-\theta_k + \Delta\theta)} \quad Given\ \theta_k < 0 \qquad [12]$$

For each branch object where an intersection could occur, the following radial sweep takes place

$$r_j = r_{j-1} + \Delta r \quad with\ r_1 \le r_j \le r_P \qquad [13]$$

In each position defined by y_i θ_k r_j, the existence of the exact intersection between the laser beam and the branch object will need to be verified. The laser beam is defined by the position y_i, θ_k, r_j and the elementary increases of Δy, $r\Delta\theta$, Δr.

3 Interaction between the laser beam and the virtual orchard

In a sweep-carried process, the end of the laser beam has a discreet minimum volume ($\Delta y \cdot r\Delta\theta \cdot \Delta r$). The intersection of each laser beam with a tree branch has also been evaluated. Due to the position of the cross-sectional advance (y_i) and the angle of simple scan (θ_k), a complete radial route takes place (from the values r_1 to r_P). For each radial position r_j ($r_1 \le r_j \le r_P$), SIMLIDAR is able to obtain the geometric characteristics of the laser beam and compares them to all the objects of the tree. Since the search extends from 1 to n, where n is the total number of branches in the model, an intersection occurs between the parallelepiped laser beam outline and the outline of each branch. In order to improve the timing of the process, SIMLIDAR obtains a verification before the intersection outline.

3.1 Dot matrix that represents the laser beam

The modelled laser beam object is a cylindrical sector with dimensions $\Delta y \cdot r\Delta\theta \cdot \Delta r$. In this cylindrical sector, the possible intersection with the cylindrical trunk that represents the branch must be found. The laser beam cylindrical sector is reduced to a dot matrix. The intersection between the laser beam and the branch is represented by an inner point problem between the branch cylindrical sector and a point. The possibility of intersection is considered if one of the points on the dot matrix is within the branch.

The configuration of the dot matrix is based on a whole number that denominates precision (P); SIMLIDAR takes a particular precision, $P = 2$. The number of points of the matrix is $(P+1)^3$, which in the case of $P = 2$ results in a value of 27 points of verification. It has been verified empirically that there is no significant change in the simulation results when P changes from a value of 2 to a value of 3; for this reason the lower value is adopted. The coordinates can be represented as a cubic matrix that has a dimension of $P+1$. The index of the elements of the dot matrix is shown as superscript; the letters of the index are *a*, *b*, *c*. A generic element of the dot matrix is $(x \quad y \quad z)^{a,b,c} = (x^{a,b,c} \quad y^{a,b,c} \quad z^{a,b,c})$ with $1 \le a \le P+1$, $1 \le b \le P+1$ and $1 \le c \le P+1$. The value of a generic point of the matrix is:

$$x^{a,b,c} = x_0 + \left(r_j + (c-1) * \frac{\Delta r}{P} \right) * \sin\left(\theta_k + (b-1) * \frac{\Delta \theta}{P} \right)$$

$$y^{a,b,c} = y_i + (a-1) * \frac{\Delta y}{P} \qquad [14]$$

$$z^{a,b,c} = z_0 + \left(r_j + (c-1) * \frac{\Delta r}{P} \right) * \cos\left(\theta_k + (b-1) * \frac{\Delta \theta}{P} \right)$$

where (x_0, z_0) is the origin axis of the LIDAR and (y_i, θ_k, r_j) is the current laser beam position.

3.2 Inner Point to a cylindrical trunk

In SIMLIDAR an intersection between the laser beam and a branch occurs when one of the points of the matrix $(x \quad y \quad z)^{a,b,c}$ intersects with one of the cylindrical trunks that represents a branch set. A point $(x \quad y \quad z)^{a,b,c}$ which is within the trunk cylinder must fulfil the following two conditions. First, the point $(x \quad y \quad z)$ must be found within the region of A^3 relative to the planes which are orthogonal to the axis of the cylinder (π_1 and π_2) and which pass through the end points $(x_1 \quad y_1 \quad z_1)$ and $(x_2 \quad y_2 \quad z_2)$. Second, the distance from $(x \quad y \quad z)$ to the axis of the cylinder must be smaller than or equal to the radius *r*.

4 SIMLIDAR parameters

The L-System process for plant modelling can be managed with several parameters. The various parameters correspond to different orchard models. These parameters are:

- *Type of tree*: in this work, the type of tree is set to "Apple", but it would be possible to select other virtual plant models (for example, vineyard). The L-System grammar used depends on these parameters.
- *Number of iterations*: the maximum number of generations or times that the axiom is replaced with the production rules.
- *Angle*: the value in degrees that increases or decreases as the turtle heads through the $\vec{L}$ axis with the commands + and –.

- *Rotation*: the value in degrees that increases or decreases as the turtle heads through the $\vec{U}$ axis with the commands T and t.
- *Diameter of the smallest branch*: the diameter of the minimum branch order according to the biological terminology (de Reffye et al., 1988).
- *Number of trees in the orchard*: the number of trees generated in the orchard. If the stochastic option is selected, all the trees will be different.
- *Pruning*: if pruning is selected, all the down-sloping branches will be removed from the plant model.
- *Stochastic*: if the stochastic option is selected, a set of probabilistic productions are used in the L-System grammar.

In addition, SIMLIDAR can manage the precision of the scanning process by means of the following parameters:

- *Laser beam position*: this allows the $(x_0 \quad z_0)$ axis position along which the virtual scanner is moving to be set.
- *Cross-sectional advance increase*: this allows the distance interval that increases the *y* position of the scanner to be set.
- *Angular advance increase*: sets the angular interval (in degrees) that increases the θ position of the scanner.
- *Distance along the laser beam increase*: sets the distance interval that increases the *r* position of the laser beam. It is the resolution in determining intersections along the laser beam.
- *Gap parameter*: allows a gap to be set in the cross-sectional advance in which the scanner process is omitted. If it has 0 value, a full scan is done. Jumps are simulated in the scan, in order to allow the tractor to move forward without scanning over the orchard in this particular cross-sectional advance. This parameter tidies up the combined effect of tractor forward speed and scanning speed. Scanning speed is zero in the virtual simulation and the forward speed has no impact, with the gap parameter replacing both.

5 Tests to evaluate the SIMLIDAR application

Forty two different virtual orchards have been developed to check different vegetative measurements relative to the 2D scanning results. To configure the plant geometry, we used the following grammar and interpretation parameters:

- Number of iterations: 4, 5, 6, 7
- Angle: 20º
- Rotation: 20º
- Diameter of the smallest branch: 5, 6 and 7
- Number of trees in the orchard: 1 and 4
- Pruning and not pruning
- Stochastic and non-stochastic

The parameters used in the scanning process were:

- Laser beam axis position: x_O = 1 m, y_O = 1 m

- Cross-sectional advance increase: $\Delta y = 0.002$ m
- Radial advance increase: $\Delta r = 0.002$ m
- Angular advance increase: $\Delta\theta = 0.25^{o}$

RESULTS AND DISCUSSION

In the simulations performed, a good linear correlation has been found between A_{IM}, A_{PR} and A_L (Fig 5 and 6):

$$\begin{aligned} A_{PR} &= 3.6166 \cdot A_{IM} \ (\text{with } R^2 = 0.7002) \\ A_L &= 10.812 \cdot A_{IM} \ (\text{with } R^2 = 0.7756) \end{aligned} \quad [15]$$

The impacted area measures the sum of all the discrete laser beam impacts as the virtual tractor-mounted LIDAR (cross-section and angular) advances. The resulting area is the area which can be measured by means of the laser tractor-mounted scanning in real orchards. The projected area is the maximum area that can be impacted by the laser beam. It will coincide with the impacted area when branches are orthogonal to the laser beam. As a result, the projected area is always greater than the impacted area. If a part of a branch is hidden by another branch, its area will not be added to the impacted area, but is added to the projected area.

The virtual orchard model allows these four parameters to be measured with precision in a variety of different kinds of orchards, with varying growth patterns. The correlation which was found can be used to estimate the measurements in a real orchard where a tractor-mounted LIDAR scanning has been applied.

A performance test was carried out using a laptop (Samsung model Q310E) with an Intel(R) Core(TM)2 Duo CPU 2.00 GHz processor, a 4GB (2,99 GB available) memory and a Windows 7 (32 bits) operating system. The results of this test are summarised in Table 3. The performance can be considered excellent given the number of branches and scanning steps which can be managed on a standard laptop.

According to the results obtained, the L-System has shown its effectiveness in producing virtual tree wood structures. When representing the tree leaf distribution, L-System productions need to adjust the pattern of leaves facing the sun to match reality, so that the foliage density is higher in the outer layer.

SIMLIDAR achieves a full and precise scan of a virtual plant model. Even though the stochastic laser beam impact is not considered, SIMLIDAR only requires a short processing time to obtain the expected measurements of a full orchard scanner. In addition, the gap parameters of SIMLIDAR can be used to simulate a non-continuous scanning process. SIMLIDAR is suitable for testing the ability of a computer utility library to process an experimental LIDAR orchard scan. In addition, SIMLIDAR can help in testing various numerical library layers of the full program, in the event that a computer system needs to be developed which can obtain a 3D structure of an orchard from a previous LIDAR scan. This particular aspect of SIMLIDAR could potentially enable the omission of some of the more tedious experimental measurements for real orchards.

For the next version of SIMLIDAR we intend to study the leaves in the grammar interpretation of the virtual orchard. We will also consider other kinds of tree crops, such as vineyard, as well as airborne LIDAR simulation.

Use of this software could also facilitate development of new computer libraries to scan real orchards, with the possibility of unit testing of these libraries. These tests can be separated from the variability of the sensor interacting with the environment. The user will have a snapshot of an orchard model which could be used to repeat a process as many times as necessary.

CONCLUSIONS

SIMLIDAR is an object-oriented application that initially generates an artificial orchard using a Lindenmayer system (L-System). Subsequently, it simulates the lateral interaction between a terrestrial laser scanner (LIDAR) and the virtual orchard.

In the application of SIMLIDAR to different leafless orchards (apple trees), a good correlation was found between the projected wood area of virtual trees and the area detected by LIDAR (R^2=0.7002). Also, a satisfactory relationship (R^2=0.7756) was found between the area detected by LIDAR and the total wood area of the tree. These good correlations support the precision of the scan simulation. Furthermore, SIMLIDAR has a quick processing time. LIDAR simulation is a process which is independent of the L-system geometry used, and has proven to be quite satisfactory according to the obtained results.

REFERENCES

Abelson, H. & diSessa, A. Turtle Geometry. (1982). M.I.T. Press, Cambridge.

Arnó, J., Vallès, J.M., Llorens, J., Blanco, R., Palacín, J., Sanz, R., Masip, J., Ribes-Dasi, M., & Rosell, J.R. (2006). Ground laser scanner data analysis for Leaf Area Index (LAI) prediction in orchards and vineyards. XVI CIGR World Congress - AgEng Bonn 2006 - 64th VDI-MEG International Conference Agri-cultural Engineering - FAO Workshop Global Issues, Bonn, CD-ROM, Paper 214.

Barawid Jr., O.C., Mizushima, A., Ishii, K., & Noguchi, N. (2007). Development of an autonomous navigation system using a two-dimensional laser scanner in an orchard application. Biosystems Engineering, 96 (2), 139-149.

Brandtberga, T., Warnera, T.A., Landenbergerb, R.E., & McGrawb, J.B. (2003). Detection and analysis of individual leaf-off tree crowns in small footprint, high sampling density lidar data from the eastern deciduous forest in North America. Remote Sensing of Environment, 85 (3), 290-303.

Chateau, T., Debain, C., Collange, F., Trassoudaine, L., & Alizon, J. (2000). Au-tomatic guidance of agricultural vehicles using a laser sensor. Computers and Electronics in Agriculture, 28, 243-257.

Chomsky, N. (1956). Three models for the description of language. IRE Trans. on Information Theory, 2(3):113–124.

Costes, E., Smith, C., Renton, M., Guédon, Y., Prusinkiewicz, P., & Godin, C. (2008). MAppleT: simulation of apple tree development using mixed stochastic and biomechanical models. Functional Plant Biology, 2008, 35, 936-950.

574 DeFries RS, Townshend JRG, & Hansen MC. (1999). Continuous fields of vegetation
575 characteristics at the global scale at 1-km resolution. Journal of Geophysical
576 Research 104(D14): 16911–16923.
577 Frijters, D., & Lindenmayer A. (1974). A model for the growth and flowering of Aster
578 novae-angliae on the basis of table (1,0) L systems. In G. Rozenberg and A.
579 Salomaa, editors, L Systems, Lecture Notes in Computer Science 15, pages 24–
580 52. Springer-Verlag, Berlin.
581 Henning, J.G., & Radtke, P.J. (2006). Detailed Stem Measurements of Standing Trees
582 from Ground-Based Scanning Lidar, 52 (1), 67-80.
583 Holmgren, J., & Persson A. (2004). Identifying species of individual trees using
584 airborne laser scanner. Remote Sensing of Environment, 90 (4), 415-423.
585 Hosoi, F., Yoshimi, K., Shimizu, Y., & Omasa, K. (2005). 3-D measurement of trees
586 using a portable scanning lidar. Phyton ISSN 0079-2047, 45 (4), 497-500.
587 Hosoi, F., & Omasa, K. (2006). Voxel-Based 3-D Modeling of Individual Trees for
588 Estimating Leaf Area Density Using High-Resolution Portable Scanning Lidar.
589 Geoscience and Remote Sensing, 44 (12), 3610 - 3618.
590 Kim, A.M. (2009). Simulating full-waveform LIDAR. Thesis (PhD). Naval
591 Postgraduate School. Monterey, California.
592 Lee, K.H., & Ehsani, R. (2007). Comparison of two 2D laser scanners for sensing object
593 distances, shapes and surface patterns. Computers and Electronics in
594 Agriculture, article in press, doi:10.1016/j.compag.2007.08.007.
595 Lefsky, M.A., Cohen, W.B., Acker, S.A., Parker, G.G., Spies, T.A., & Harding, D.
596 (1999). Lidar Remote Sensing of the Canopy Structure and Biophysical
597 Properties of Douglas-Fir Western Hemlock Forests. 70 (3), 339-361.
598 Lindenmayer, A. (1968). Mathematical models for cellular interaction in development,
599 Parts I and II. Journal of Theoretical Biology, 18:280–315.
600 Maltamo, M., Eerikäinen K., Pitkänen, J., Hyyppä, J., & Vehmas, M. (2004).
601 Estimation of timber volume and stem density based on scanning laser altimetry
602 and expected tree size distribution functions. Remote Sensing of Environment,
603 90 (3), 319-330.
604 Mizrach, A., Shmulevich, I., Yekutieli, O, & Edan, Y. (1994). Evaluation of a laser
605 method for guidance of field machinery. Computers and Electronics in
606 Agriculture, 10, 135-149.
607 Monta, M., Namba, K., & Kondo, N. (2004). Three dimensional sensing system using
608 laser scanner. ASAE/CSAE Paper No. 041158, St. Joseph, MI, USA.
609 OpenGL. 1997. OpenGL organization. Gold Standard Group.
610 Omasa, K., Hosoi, F., & Konishi, A. (2007). 3D lidar imaging for detecting and
611 understanding plant responses and canopy structure. Journal of Experimental
612 Botany, 58 (4), 881-898.
613 Palacín, J., Pallejà, T., Tresánchez, M., Sanz, R., Llorens, J., Ribes-Dasi, M., Masip, J.,
614 Arnó, J., Escolà, A., & Rosell, J.R. (2007). Real-time tree-foliage surface
615 estimation using a ground laser scanner. IEEE Transactions on Instrumentation
616 and Measurement, 56 (4), 1377-1383.
617 Parker, G., Harding, J., & Berger, M. (2004). A portable LIDAR system for rapid
618 determination of forest canopy structure. Journal of Applied Ecology, 41 (4),
619 755-767.
620 Prusinkieweicz, P. (1987). Applications of L-Systems to computer imagery, Graph
621 Grammars and their Aplication to computer Science; Third International
622 Workshop, Ehrig H., Nagl M., Rosenfeld A. & Rozenberg G. (eds), pp. 534-548.

623 Prusinkiewicz, P., Lindenmayer, A., & Hanan, J.. (1988). Developmental models of
624 herbaceous plants for computer imagery purposes. Proceedings of SIGGRAPH
625 '88 (Atlanta, Georgia, August 1-5, 1988), in Computer Graphics 22,4 (August
626 1988), pages 141–150, ACM SIGGRAPH, New York.
627 Prusinkiewicz, P., & Hanan, J. (1990 a). Visualization of botanical structures and
628 processes using parametric L-systems. In D. Thalmann, editor, Scientific
629 Visualization and Graphics Simulation, pages 183–201. J. Wiley & Sons
630 Prusinkiewicz, P., & Lindenmayer, A. (1990). The algorithmic beauty of plants.
631 Springer Verlag, New York.
632 Prusinkiewicz, P., Karwowski, R., Měch, R., & Hanan, J. (2000). L-Studio/cpfg: A
633 Software System for Modeling Plants. Lecture Notes in Computer Science,
634 2000, Volume 1779/2000, 161-164.
635 de Reffye, P., Edelin, C., Jaeger, M., & Puech, C. (1988). Plant models faithful to
636 botanical structure and development. *Computer Graphics, 22,* 151–158.
637 Riaño, D., Chuvieco, E.Condés, S., González-Matesanz, J., & Ustin, S.L. (2004).
638 Generation of crown bulk density for Pinus sylvestris L. from lidar. Remote
639 Sensing of Environment, 92 (3), 345-352.
640 Rogelberg, D. (1992). OpenGL Reference Manual, Addison-Wesley, Reading, MA. 16.
641 Rosell, J.R., Llorens, J., Sanz, R., Arno, J., Ribes-Dasi, M., Masip, J., Escola, A., Camp,
642 F., Solanelles, F., Gracia, F., Gil, E., Val, L., Planas, S., & Palacin, J. (2009a).
643 Obtaining the three-dimensional structure of tree orchards from remote 2D
644 terrestrial LIDAR scanning. Agricultural and Forest Meteorology 149 (9), 1505–
645 1515.
646 Rosell, J.R., Sanz, R., Llorens, J., Arno, J., Escola, A., Ribes-Dasi, M., Masip, J., Camp,
647 F., Gracia, F., Solanelles, F., Pallejà, T., Val, L., Planas, S., Gil, E., & Palacín, J.
648 (2009b). A tractor mounted scanning LIDAR for the non-destructive
649 measurement of vegetative volume and surface area of tree-row plantations: a
650 comparison with conventional destructive measurements. Biosystems
651 Engineering 102 (2), 128–134.
652 Sipser, M. (1997). Introduction to the Theory of Computation. PWS Publishing
653 Company, 1997
654 Subramanian, V., Burks, T.F. & Arroyo, A.A. (2006). Development of machine vision
655 and laser radar autonomous vehicle guidance systems for citrus grove
656 navigation. Computers and Electronics in Agriculture, 53, 130-143.
657 Tarquis, A., & González-Andrés, F. (1995). Stochastic L-system Applied to the
658 Calculation of the Leaf Area of a Shrubby Legume for Forage (Chamaecytisus
659 rathenicus, F. ex Wol.). In: M.N. Novak (Editor), Fractal Reviews in the Natural
660 and Applied Sciences, Chapman and Hall, 192-203.
661 Tarquis, A.M., Méndez, V., Walklate, P.J., Castellanos, M. T., & Morató, M. C. (2006).
662 L-system tree model and LIDAR simulator: estimation of spray target area.
663 WSEAS TRANSACTIONS on BIOLOGY and BIOMEDICINE. Vol 3 Nº 2 81-
664 88. ISSN 1109-9518.
665 Tucker, C.J., Vanpraet, C.L., Sharman, M.J., & Van Ittersun, G. (1985). "Satellite
666 remote sensing of total herbaceous production in the Senegalese Sahel 1980-
667 1984", Rem. Sens. Environ., 17, 232-249.
668 Tumbo, S.D, Salyani, M., Whitney J.D., Wheaton T.A., & Miller W.M. (2002).
669 Investigation of laser and ultrasonic ranging sensors for measurements of citrus
670 canopy volume. Applied Engineering in Agriculture, 18(3), 367–372.
671 Von Koch, H. (1905). Une méthode géométrique élémentaire pour l'étude de certaines
672 questions de la théorie des courbes planes. Acta mathematica, 30:145–174.

673 Walklate, P.J., Richardson G.M., Baker, D.B., Richards, P.A., & Cross, J.V. (1997).
674 Short range LIDAR measurement of top fruit tree canopies for pesticide
675 applications research in the UK. Proceedings of SPIE - International Society for
676 Optical Engineering Advances in Laser Remote Sensing for Terrestrial and
677 Oceanographic Application, Orlando, Florida, Vol. 3059, 143-151.
678 Walklate, P.J., Cross, J.V., Richardson, G.M., Murray, R.A., & Baker, D.E. (2002).
679 Comparison of different spray volume deposition models using LIDAR
680 measurements of apple orchards. Biosystems Engineering 82 (3), 253-267.
681 Wei, J, & Salyani, M. (2004). Development of a laser scanner for measuring tree
682 canopy characteristics: Phase I. Prototype development. Transactions of the
683 ASAE, 47(6), 2101–2107.
684 Wei, J., & Salyani, M. (2005). Development of a laser scanner for measuring tree
685 canopy characteristics: Phase 2. Foliage density measurement. Transactions of
686 the ASAE, 48 (4), 1595-1601.
687
688
689 ## Table Captions
690 • **Table 1**: Non-stochastic apple tree derivation string (for 2 and 3 generations).
691 • **Table 2**: L-System alphabet used.
692 • **Table 3**: Performance of the scan process. This test was carried out using a
693 Samsung laptop model Q310. Processor: Intel(R) Core(TM)2 Duo CPU 2.00 GHz.
694 Memory: 4GB (2.99 GB available). Operative system: Windows 7, 32 bits.
695
696 ## Figure Captions
697 • **Figure 1**: The order of axes (from Reffye, 1998, p.152).
698 • **Figure 2**: Three dimensional orchard model (lateral view) and its two dimensional
699 scan simulation. In two-dimensional scan the dimension in height and width depend
700 on value of cross-section increase (Δy) and angular advance increase ($\Delta\theta$), the
701 final dimension could be different to three dimensional view. In two-dimensional
702 scan the color is selected depending on the measured distance in scan (l_{ij}).
703 • **Figure 3**: Projected wood area.
704 • **Figure 4:** Angular advance (θ_1 to θ_M) for a y_i cross-section position. Angular
705 sweeping (r_1 to r_P) for a y_i cross-section and θ_K angular position.
706 • **Figure 5:** A_{PR} – Projected area (m^2) vs A_{IM} – Impacted area (m^2).
707 $A_{PR} = 3.6166 \cdot A_{IM}$ with $R^2 = 0.7002$.
708 • **Figure 6:** A_L – Wood area (m^2) *vs* A_{IM} – Impacted area (m^2). $A_L = 10.812 \cdot A_{IM}$ with
709 $R^2 = 0.7756$.
710
711
712
713
714
715
716
717
718
719
720

Table 1 .- Non-stochastic apple tree derivation string (for 2 and 3 generations)

i^{th} generation	Derivation string	Three dimensional representation
2	[I01I01[t+I01I01+I02I02[t+I02I02+F]I02[T-I02F]I02F]I01[T-I01I02I02[t+I02I02+F]I02[T-I02F]I02F]I01I02I02[t+I02I02+F]I02[T-I02F]I02F]	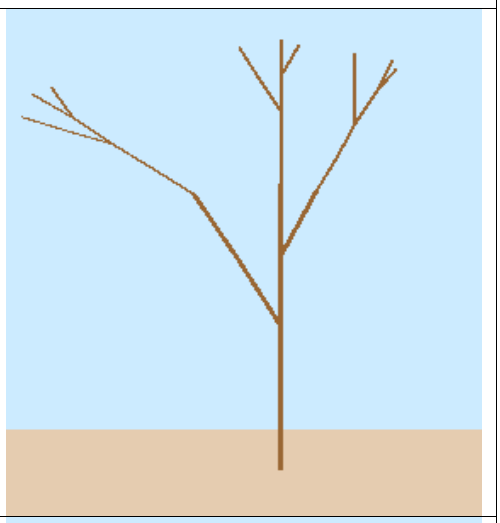
3	[I01I01[t+I01I01+I02I02[t+I02I02+I03I03[t+I03I03+F]I03[T-I03F]I03F]I02[T-I02I03I03[t+I03I03+F]I03[T-I03F]I03F]I02I03I03[t+I03I03+F]I03[T-I03F]I03F]I01[T-I01I02I02[t+I02I02+I03I03[t+I03I03+F]I03[T-I03F]I03F]I02[T-I02I03I03[t+I03I03+F]I03[T-I03F]I03F]I02I03I03[t+I03I03+F]I03[T-I03F]I03F]I01I02I02[t+I02I02+I03I03[t+I03I03+F]I03[T-I03F]I03F]I02[T-I02I03I03[t+I03I03+F]I03[T-I03F]I03F]I02I03I03[t+I03I03+F]I03[T-I03F]I03F]	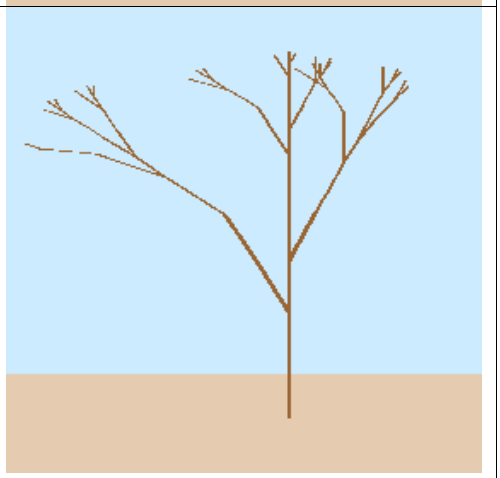

Table 2 .- L-System alphabet used.

Variable	Interpretation	Turtle Command
F	Leaf	Insert a closed polygonal at turtle location oriented through heading $\vec{H}$.
I	Node without bud	Moves turtle a fixed straight line
[	Beginning of Branch	Store the current state of the turtle (location and heading $\vec{H}$)
]	End of Branch	The branch is completed and the turtle return to previous state stored
+	Upwards Roll	Roll the turtle heading clockwise, increasing the current $\vec{L}$ angle.
-	Downwards Roll	Roll the turtle heading counter-clockwise, decreasing the current $\vec{L}$ angle.
T	Increase of Turn	Turn the turtle heading increasing the current $\vec{U}$ angle.
t	Decrease of Turn	Turn the turtle heading decreasing the current $\vec{U}$ angle.

Table 3.- Performance of the scan process. This test was carried out using a Samsung laptop model Q310. Processor: Intel(R) Core(TM)2 Duo CPU 2.00 GHz. Memory: 4GB (2.99 GB available). Operative system: Windows 7, 32 bits.

Nº iterations	**Nº trees**	**Total of branchs**	**Dimension N×M of scan**	**Scan process time (in min.)**
4	1	360	558,930	2
5	1	1,497	561,935	4
6	1	5,564	504,840	11
7	1	15,168	579,965	26
4	2	928	931,550	6
5	2	3,056	1,063,770	12
6	2	10,415	1,039,730	31
7	2	29,779	1,319,195	96
4	3	1,011	1,271,115	7
5	3	5,112	1,550,580	24
6	3	15,229	1,562,600	61
7	3	48,250	1,571,615	174
4	4	2,064	1,634,720	15
5	4	4,991	2,482,130	32
6	4	20,020	2,404,000	135
7	4	44,658	2,467,105	210

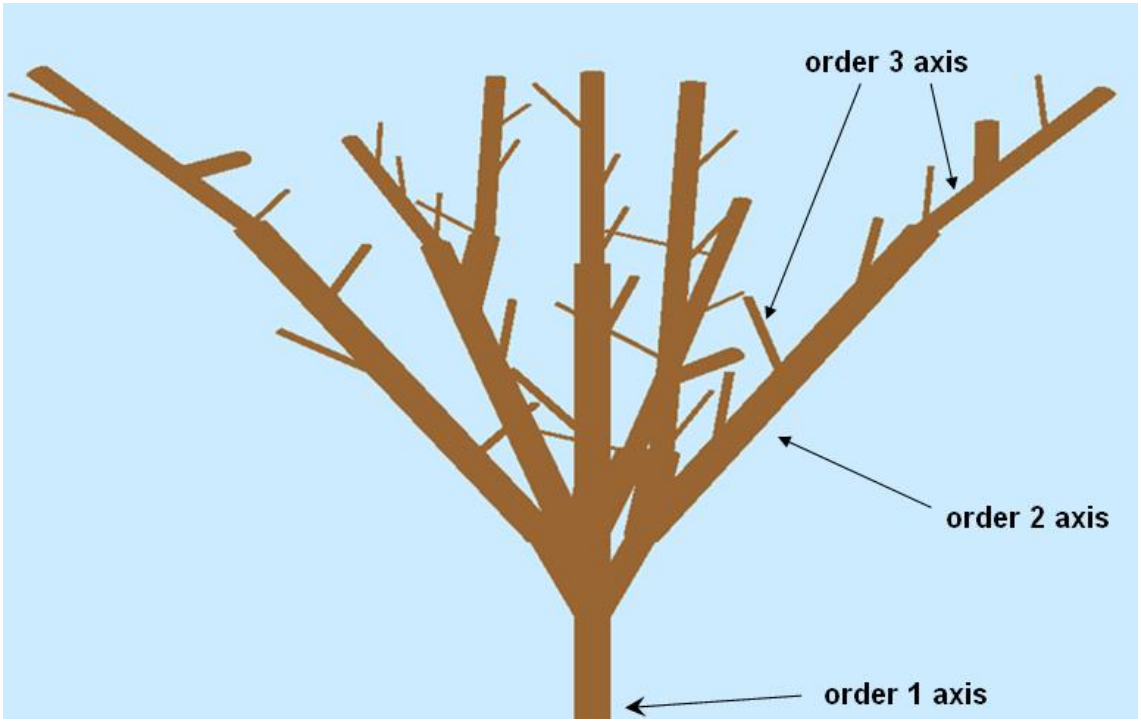

Figure 1.- The order of axes (from Reffye, 1998, p.152)

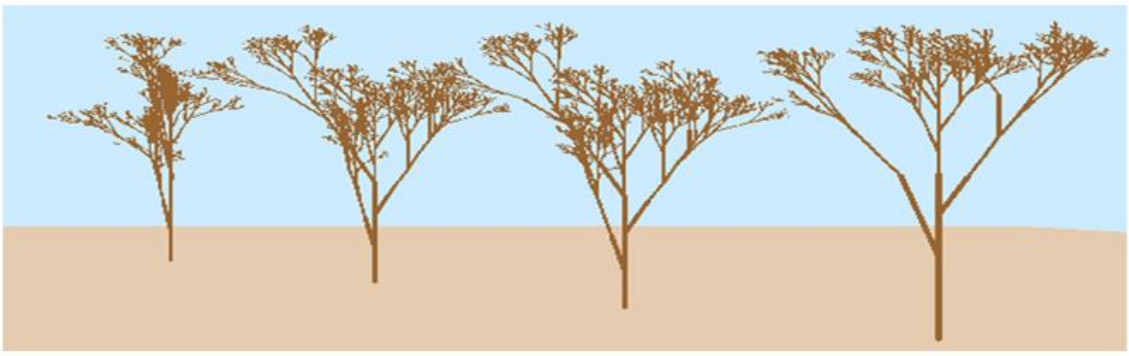

a) 3D orchard model. Lateral view.

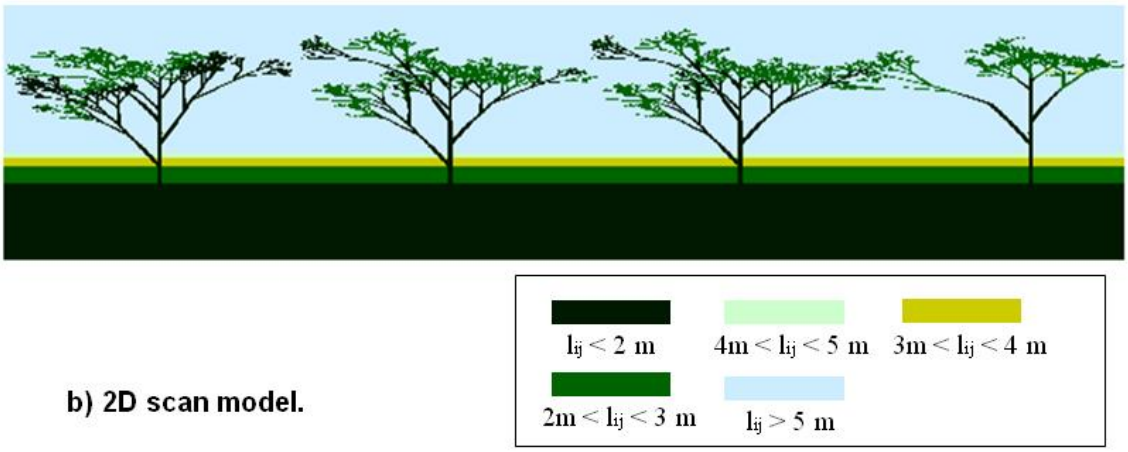

b) 2D scan model.

Figure 2.- Three dimensional orchard model (lateral view) and its two dimensional scan simulation. In two-dimensional scan the dimension in height and width depend on value of cross-section increase (Δy) and angular advance increase ($\Delta\theta$), the final dimension could be different to three dimensional view. In two-dimensional scan the color is selected depending on the measured distance in scan (l_{ij}).

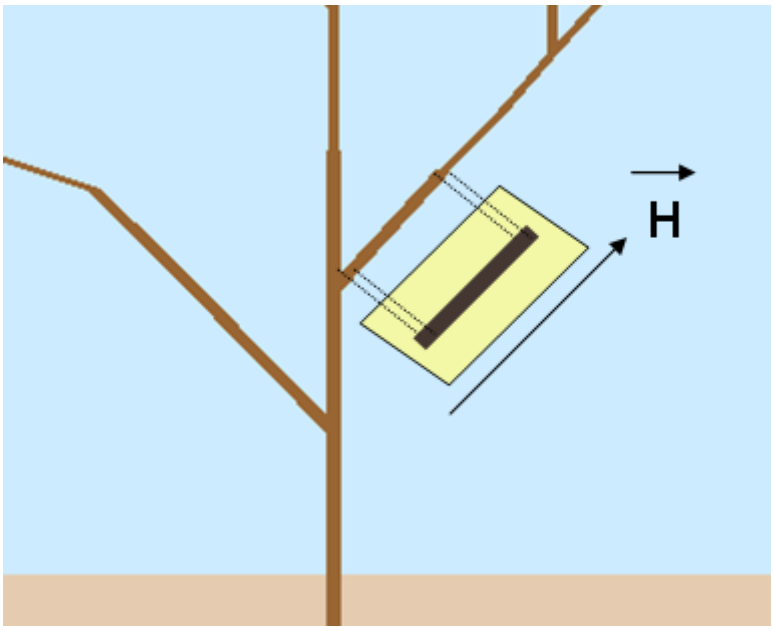

Figure 3.- Projected wood area.

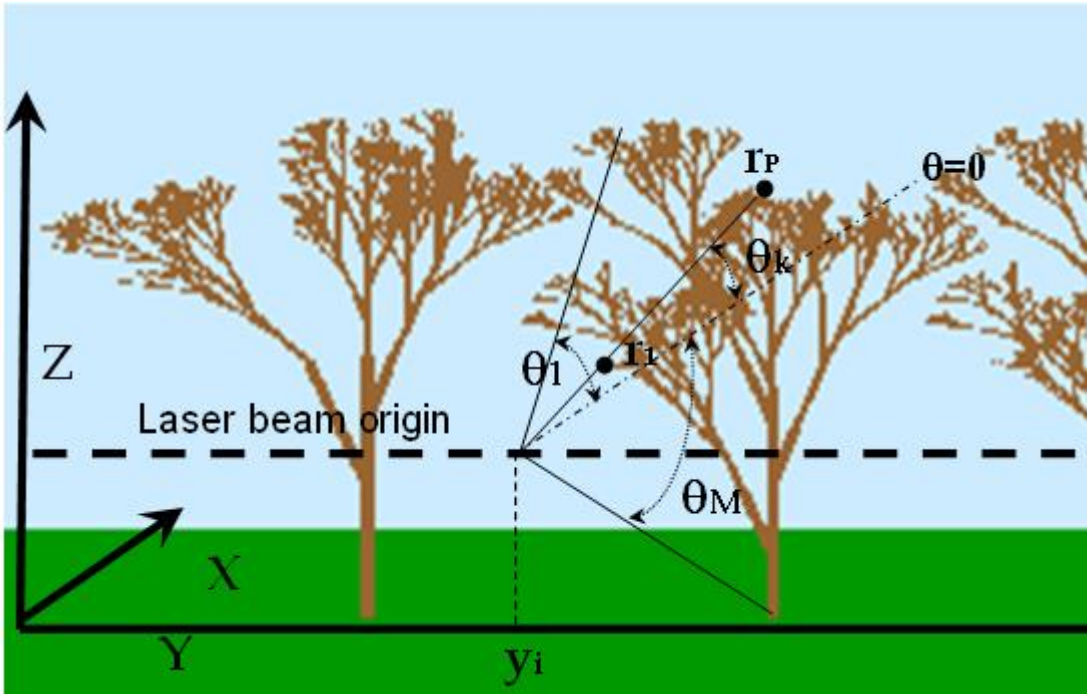

Figure 4.- Angular advance (θ_1 to θ_M) for a y_i cross-section position.
Angular sweeping (r_1 to r_P) for a y_i cross-section and θ_K angular position.

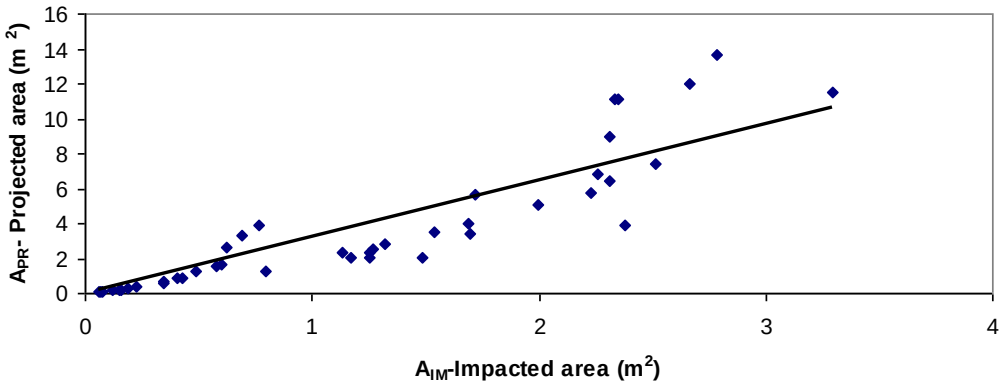

793
794 Figure 5.- A_{PR} – Projected area (m^2) vs A_{IM} – Impacted area (m^2). $A_{PR} = 3.6166 \cdot A_{IM}$
795 with $R^2 = 0.7002$.
796

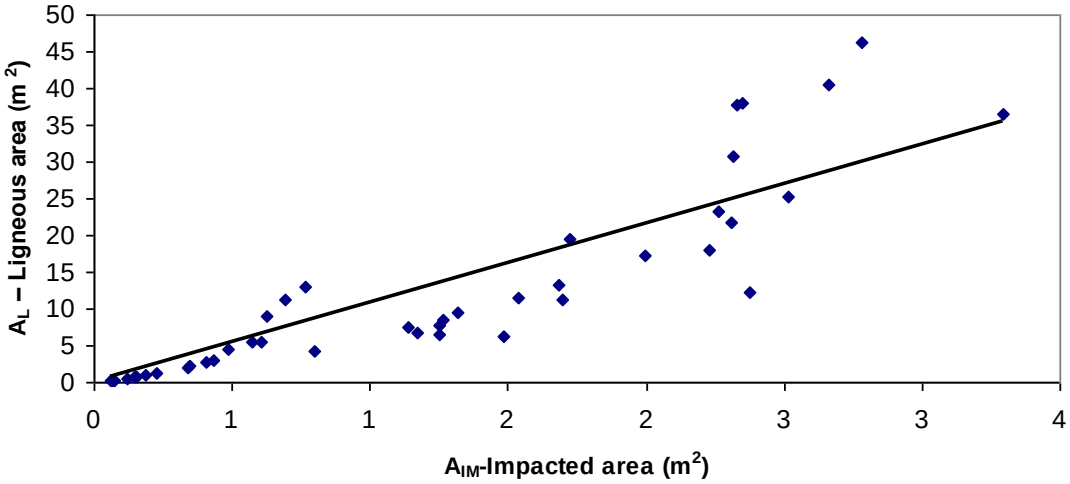

797
798 Figure 6.- A_L – Wood area (m^2) *vs* A_{IM} – Impacted area (m^2). $A_L = 10.812 \cdot A_{IM}$ with
799 $R^2 = 0.7756$.
800